TECHNISCHE MECHANIK, Band 17, Heft 4, (1997), 307-312
Manuskripteingang: 02. Juni 1997

The Impact of Laminate Surface Cracks on Surface Quality

W. Becker

Within a thermally loaded $[90°/0°]_S$-cross-ply laminate a transverse matrix crack in the upper ply is considered as an idealized model defect. With the crack emergence the laminate does not remain dimensionally stable, but due to a redistribution of local stresses some corresponding laminate deformation occurs. The analysis of the crack resultant laminate deformation can be performed by a higher order laminate theory specially formulated for that purpose. For an appropriately chosen set of kinematic variables the consideration of stress equilibrium leads to a system of differential equations which can be solved in a closed-form manner. The corresponding solution includes the representation of all deformation aspects and in particular allows to quantify the resultant effective laminate surface roughness.

1 Introduction

Within the last years CFRP (carbon fiber reinforced plastic) laminates have demonstrated their usefulness also for such lightweight applications where an extremely high dimensional stability is needed. Important examples for that are thermally loaded mirror carriers for antenna reflectors where the surface smoothness has to meet optical quality requirements (Salmen et al., 1993; Ehmann et al., 1994). Typically the operating temperature of a CFRP laminate is well below the curing temperature. Then due to the anisotropic thermal expansion properties of unidirectional CFRP plies a laminate gets thermally prestressed. In general the coefficient of thermal expansion is close to zero in fiber direction (or even slightly negative), whereas in transverse direction it is clearly positive and of a significant magnitude. For the laminate below curing temperature in the individual unidirectional ply this leads to compressive stress in fiber direction and to tension stress in transverse direction. Thus transverse matrix cracks are prone to develop. If a matrix crack actually evolves, its crack faces become stress-free and thus local stresses are released with the opening of the crack. Then the main detrimental effect is not just the crack opening (appearing as a scratch on the laminate surface) but it is the accompanying redistribution of cross-sectional forces and the resultant laminate deformation. This deformation and the corresponding surface degradation are to be analysed in the following.

2 The Problem Considered and its Analysis

As an idealized model defect situation the case of a $[90°/0°]_S$-cross-ply laminate is considered, where for a negative temperature load $\Delta T < 0$ (i.e. operating temperature below curing temperature) a matrix crack has developed in the upper 90°-ply, as it is schematically shown in Figure 1.

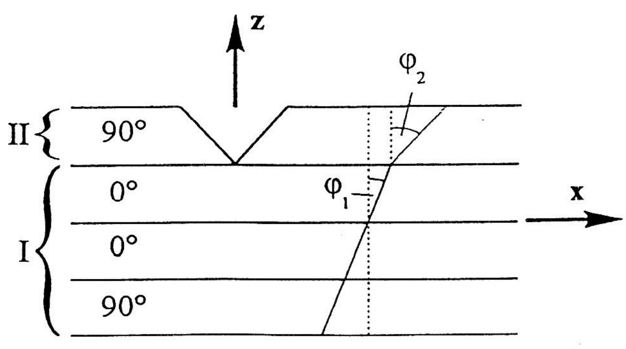

Figure 1. Idealized Model Defect Situation

For the analysis it is appropriate to consider the three lower intact plies together as a sublaminate I whereas the upper 90°-ply is considered as a sublaminate II. For an idealized representation of the displacement field within the laminate four kinematic variables are introduced which are pure functions of x, namely the displacements $u_0(x)$ and $w(x)$ of the laminate midplane in x- and z-direction and the deflection angles $\varphi_1(x)$ and $\varphi_2(x)$ of the respective sublaminates I and II. By means of the functions introduced the displacement field within the whole laminate continuum (sublaminates I and II) can be represented as follows:

$$
\begin{aligned}
u(x,z) &= \begin{cases} u_0(x) + z\varphi_1(x) & \text{for} \quad z \leq \frac{h}{4} \\ u_0(x) + \frac{h}{4}\varphi_1(x) + (z - \frac{h}{4})\varphi_2(x) & \text{for} \quad \frac{h}{4} \leq z \leq \frac{h}{2} \end{cases} \\
w(x,z) &= w(x)
\end{aligned}
\tag{1}
$$

According to the standard strain-displacement relations the displacements (1) give the following strains:

$$
\begin{aligned}
\varepsilon_x &= \begin{cases} u_0' + z\varphi_1' & \text{for} \quad z \leq \frac{h}{4} \\ u_0' + \frac{h}{4}\varphi_1' + (z - \frac{h}{4})\varphi_2' & \text{for} \quad \frac{h}{4} \leq z \leq \frac{h}{2} \end{cases} \\
\gamma_{xz} &= \begin{cases} w' + \varphi_1 & \text{for} \quad z \leq \frac{h}{4} \\ w' + \varphi_2 & \text{for} \quad \frac{h}{4} \leq z \leq \frac{h}{2} \end{cases}
\end{aligned}
\tag{2}
$$

From the strains (2) with Hooke's law the following inplane stresses σ_x and σ_y occur in the individual laminate plies:

$$
\begin{bmatrix} \sigma_x \\ \sigma_y \end{bmatrix} = \begin{bmatrix} \overline{Q}_{11} & \overline{Q}_{12} \\ \overline{Q}_{12} & \overline{Q}_{22} \end{bmatrix} \begin{bmatrix} \varepsilon_x - \varepsilon_x^T \\ \varepsilon_y - \varepsilon_y^T \end{bmatrix}
\tag{3}
$$

Herein the quantities $\overline{Q}_{ij}$ are the standard reduced inplane stiffnesses (Jones, 1975; Tsai and Hahn, 1980), ε_x^T and ε_y^T are the thermal strains in x and y-direction, respectively, and ε_y is supposed to be constant in accordance with the underlying thermal loading:

$$
\varepsilon_x^T = \alpha_x \Delta T \qquad \varepsilon_y^T = \alpha_y \Delta T \qquad \varepsilon_y = \alpha_{eff}^{0°/90°} \Delta T
\tag{4}
$$

where the quantity $\alpha_{eff}^{0°/90°}$ denotes the effective coefficient of thermal expansion of the whole laminate. From the transverse shear strain γ_{xz} on the other hand respective transverse shear stresses result in an averaged sense, namely

$$
\begin{aligned}
\tau_{xz}^{I} &= (\tfrac{2}{3}G_{13}^{0°} + \tfrac{1}{3}G_{13}^{90°})(w' + \varphi_1) & \text{for} \quad z \leq \tfrac{h}{4} \\
\tau_{xz}^{II} &= G_{13}^{90°}(w' + \varphi_2) & \text{for} \quad \tfrac{h}{4} \leq z \leq \tfrac{h}{2}
\end{aligned}
\tag{5}
$$

The quantities $G_{13}^{0°}$ and $G_{13}^{90°}$ denote the effective shear moduli of the 0°- and 90°-plies.

For the determination of the unknown functions u_0', w', φ_1, and φ_2 use is made of the equilibrium conditions in x- and z-direction:

$$
\sigma_{x,x} + \tau_{xz,z} = 0 \tag{6}
$$

$$
\tau_{xz,x} + \sigma_{z,z} = 0 \tag{7}
$$

With the displacement field (1) the equilibrium conditions cannot be fulfilled in an identical manner at any point (x, z) of the laminate continuum, but they can be fulfilled in appropriately averaged ways.

When the equilibrium condition (6) is integrated through the whole laminate thickness from $z = -h/2$ to $z = h/2$ taking into account that the laminate is free of shear ($\tau_{xz} = 0$) at its top and bottom surfaces and that there is no resultant inplane force we have

$$\int_{-h/2}^{h/2} \sigma_x dz = 0 \tag{8}$$

When the equilibrium condition (6) first is multiplied by z and then integrated through the whole laminate thickness there results

$$\frac{d}{dx} \int_{-h/2}^{h/2} \sigma_x z dz = 0 \tag{9}$$

When the equilibrium condition (7) is integrated from $z = -h/2$ to $z = h/2$ it represents the statement of a constant resultant transverse force. In the absence of transverse loadings the resultant transverse force will be equal to zero, giving

$$\frac{3}{4} h \tau_{xz}^{I} + \frac{1}{4} h \tau_{xz}^{II} = 0 \tag{10}$$

Finally, from the equilibrium condition (6) by direct integration through the upper 90°-ply and by integration after multiplication with the thickness coordinate z the following relation can be obtained:

$$\frac{d}{dx} \int_{h/4}^{h/2} \sigma_x z dz - \frac{h}{4} \frac{d}{dx} \int_{h/4}^{h/2} \sigma_x dz - \frac{h}{4} \tau_{xz}^{II} = 0 \tag{11}$$

By means of relations (2), (3) and (5) the stresses in the (integrated) equilibrium conditions (8), (9), (10) and (11) can be traced back to the underlying deformation quantities, which eventually gives the following system of coupled differential equations:

$$\begin{bmatrix} 0 & 0 & 0 & 0 \\ 0 & 0 & A_{23} & A_{24} \\ 0 & 0 & 0 & 0 \\ 0 & 0 & A_{43} & A_{44} \end{bmatrix} \begin{bmatrix} u_0''' \\ w''' \\ \varphi_1'' \\ \varphi_2'' \end{bmatrix} + \begin{bmatrix} 0 & 0 & B_{13} & B_{14} \\ 0 & 0 & 0 & 0 \\ 0 & 0 & 0 & 0 \\ B_{41} & 0 & 0 & 0 \end{bmatrix} \begin{bmatrix} u_0'' \\ w'' \\ \varphi_1' \\ \varphi_2' \end{bmatrix} + \begin{bmatrix} C_{11} & 0 & 0 & 0 \\ 0 & 0 & 0 & 0 \\ 0 & C_{32} & C_{33} & C_{34} \\ 0 & C_{42} & 0 & C_{44} \end{bmatrix} \begin{bmatrix} u_0' \\ w' \\ \varphi_1 \\ \varphi_2 \end{bmatrix} = 0 \tag{12}$$

Within that matrix form representation the individual non-zero components in detail are:

$$\begin{aligned}
A_{23} &= \tfrac{23}{384} h^3 \overline{Q}_{11}(90^\circ) + \tfrac{1}{96} h^3 \overline{Q}_{11}(0^\circ) \qquad A_{24} = \tfrac{5}{384} h^3 \overline{Q}_{11}(90^\circ) \qquad A_{43} = \tfrac{1}{128} h^3 \overline{Q}_{11}(90^\circ) \\
A_{44} &= \tfrac{1}{192} h^3 \overline{Q}_{11}(90^\circ) \qquad B_{13} = -\tfrac{3}{32} h^2 \overline{Q}_{11}(90^\circ) + \tfrac{1}{16} h^2 \overline{Q}_{11}(0^\circ) + \tfrac{1}{16} h^2 \overline{Q}_{11}(90^\circ) \\
B_{14} &= \tfrac{1}{32} h^2 \overline{Q}_{11}(90^\circ) \qquad B_{41} = \tfrac{1}{32} h^2 \overline{Q}_{11}(90^\circ) \qquad C_{11} = \tfrac{h}{2} [\overline{Q}_{11}(90^\circ) + \overline{Q}_{11}(0^\circ)] \\
C_{32} &= 2G_{13}^{0^\circ} + 2G_{13}^{90^\circ} \qquad C_{33} = 2G_{13}^{0^\circ} + G_{13}^{90^\circ} \qquad C_{34} = 2G_{13}^{90^\circ} \\
C_{42} &= -\tfrac{h}{4} G_{13}^{90^\circ} \qquad C_{44} = -\tfrac{h}{4} G_{13}^{90^\circ}
\end{aligned} \tag{13}$$

3 Closed-Form Solution

The system of differential equations (12) is linear with constant coefficients and thus can be solved by standard methods. For the solution a representation of the kind

$$\begin{bmatrix} u_0' \\ w' \\ \varphi_1 \\ \varphi_2 \end{bmatrix} = \begin{bmatrix} U' \\ W' \\ \Phi \\ \Psi \end{bmatrix} e^{-\lambda x} \tag{14}$$

is chosen with still undetermined constants U', W', Φ, Ψ and λ. Substitution of representation (14) into the system (12) leads to an eigenvalue problem with the trivial eigenvalues $\lambda_1 = \lambda_2 = 0$ and the nontrivial eigenvalues $\lambda_3 = +\lambda$, $\lambda_4 = -\lambda$ with

$$\lambda^2 = \frac{-C_{11}C_{42}(C_{33}A_{24} - A_{23}A_{34}) - C_{11}C_{32}A_{23}C_{44}}{C_{11}C_{32}A_{23}A_{44} - C_{11}C_{32}A_{43}A_{24} + B_{41}C_{32}B_{13}A_{24} - B_{41}C_{32}A_{23}B_{14}} \tag{15}$$

The corresponding eigenvectors are

$$\begin{gathered} \begin{bmatrix} U_1' \\ W_1' \\ \Phi_1 \\ \Psi_1 \end{bmatrix} = \begin{bmatrix} U_2' \\ W_2' \\ \Phi_2 \\ \Psi_2 \end{bmatrix} = \begin{bmatrix} 0 \\ -C_{33}C_{44} \\ C_{32}C_{44} - C_{42}C_{34} \\ C_{42}C_{33} \end{bmatrix} \\ \begin{bmatrix} U_3' \\ W_3' \\ \Phi_3 \\ \Psi_3 \end{bmatrix} = - \begin{bmatrix} U_4' \\ W_4' \\ \Phi_4 \\ \Psi_4 \end{bmatrix} = \begin{bmatrix} C_{32}\lambda(B_{13}A_{24} - B_{14}A_{23}) \\ C_{11}(A_{23}C_{34} - A_{24}C_{33}) \\ C_{11}C_{32}A_{24} \\ -C_{11}C_{32}A_{23} \end{bmatrix} \end{gathered} \tag{16}$$

With that the general solution of (12) can eventually be given as

$$\begin{bmatrix} u_0' \\ w' \\ \varphi_1 \\ \varphi_2 \end{bmatrix} = (C_1 + C_2 x) \begin{bmatrix} 0 \\ W_1' \\ \Phi_1 \\ \Psi_1 \end{bmatrix} + C_3 \begin{bmatrix} U_3' \\ W_3' \\ \Phi_3 \\ \Psi_3 \end{bmatrix} e^{\lambda x} + C_4 \begin{bmatrix} U_4' \\ W_4' \\ \Phi_4 \\ \Psi_4 \end{bmatrix} e^{-\lambda x} \tag{17}$$

where the constants C_1 to C_4 are still to be determined from given boundary conditions.

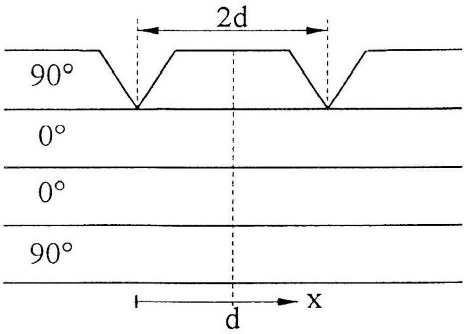

Figure 2. Periodic Crack Array Considered

Of particular practical interest is the case of neighbouring cracks that in an idealized way are arranged periodically with a characteristic distance $2d$, see Figure 2 . The corresponding boundary conditions

$$\varphi_1(0) = 0 \qquad \varphi_1(d) = 0 \qquad \varphi_2(d) = 0 \qquad \left. \int_{h/4}^{h/2} \sigma_x dz \right|_{x=0} = 0 \tag{18}$$

lead to a system of four linear equations from which C_1 to C_4 can be determined easily in a unique way.

For the assessment of the laminate deformation most important is the normal deflection w. According to the solution (17) obtained we have (after performing a simple integration for w')

$$w(x) = \left(C_1 x + C_2 \frac{x^2}{2}\right) W_1' + \frac{1}{\lambda} C_3 W_3' e^{\lambda x} - \frac{1}{\lambda} C_4 W_4' e^{-\lambda x} \tag{19}$$

As a simple indicator for the effective surface degradation the peak-to-valley value $\Delta w = w(0) - w(d)$ can be considered.

In order to assess the predictions of the analysis approach presented so far, a laminate with $h = 1\,\mathrm{mm}$ and $d = 2h = 2\,\mathrm{mm}$ and the following single ply properties is considered (T300/epoxy):

$$\begin{aligned}
E_1 &= 135000\,\mathrm{MPa} & E_2 = E_3 &= 10000\ \mathrm{MPa} \\
\nu_{12} = \nu_{23} = \nu_{13} &= 0.27 & & \\
G_{12} = G_{13} &= 5000\,\mathrm{MPa} & G_{23} &= 3972\ \mathrm{MPa} \\
\alpha_1 &= -0.6 \cdot 10^{-6}\,/\mathrm{K} & \alpha_2 &= 40 \cdot 10^{-6}\,/\mathrm{K}
\end{aligned} \tag{20}$$

From these data all other constitutive properties (as e.g. the reduced stiffnesses) can be calculated by standard relations of classical laminate theory (Jones, 1975; Tsai and Hahn, 1980).

For a temperature load of $\Delta T = -150\,\mathrm{K}$ the closed-form analysis presented yields a resultant surface degradation of $\Delta w = 1.18\,\mu\mathrm{m}$, i.e. a peak-to-valley deformation in the order of about one micron.

4 Comparison with Finite Element Analysis

In order to ensure that the derived closed-form analysis gives realistic predictions a comparative finite element analysis has been performed by means of the finite element code NASTRAN. In doing so, each laminate ply has been discretized by five layers of volume elements within the range of $x = 0...d$.

The laminate deformation (for $\Delta T = -150\,\mathrm{K}$) determined by finite element analysis in an appropriate scaling is shown in Figure 3 . The peak-to-valley value Δw results as $\Delta w = 1.33\,\mu\mathrm{m}$, which means a good agreement with the closed-form result $\Delta w = 1.18\,\mu\mathrm{m}$. Due to the kinematic assumptions introduced the closed-form model behaves somewhat stiffer than the finite element model which is not surprising. In contrast to the finite element analysis the closed-form results can be directly exploited for altered geometries (varying laminate thickness h, crack distance $2d$ etc.) and they allow to discuss parameter sensitivites in an easy way.

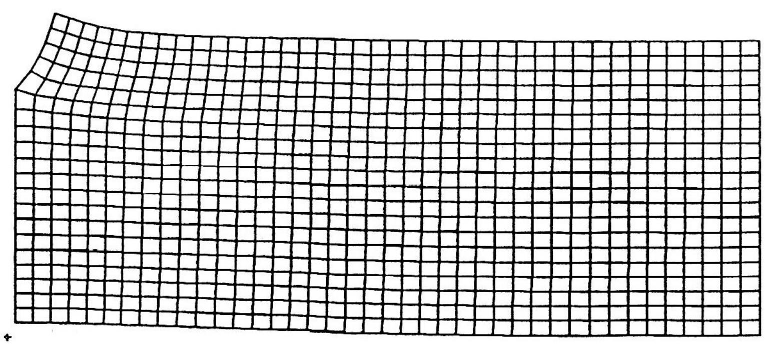

Figure 3. Deformation Determined by Finite Elements

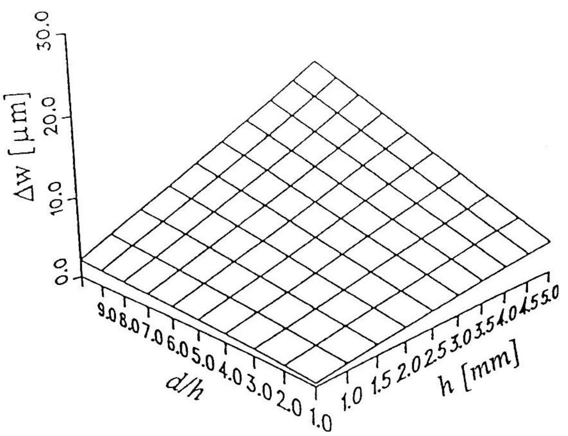

Figure 4. Surface Roughness $\Delta w(h, d/h)$

5 Discussion of Effective Surface Roughness and Conclusions

If the peak-to-valley value Δw is taken as a measure for the resultant effective surface roughness it is relatively easy to assess the corresponding surface degradation as a function of the geometrical characteristics h and d (or equivalently h and d/h). Accordingly, Figure 4 shows the resultant effective surface roughness Δw as a function of h and d/h, $\Delta w = \Delta w(h, d/h)$, for the range $h = 0.5...5$mm and $d/h = 1...10$.

It can be noted that the surface degradation Δw is the larger the larger the laminate thickness h is, and the larger the relative neighboring distance d/h is. The last statement is remarkable insofar as it means that a larger distance of the cracks to each other is more harmful than a smaller distance. On the other hand this means that in terms of the peak-to-valley value Δw the effective surface quality improves with an increasing number of surface cracks (higher crack density, smaller neighboring distance).

Thus, for a good surface smoothness it is desirable either to have no surface cracks or to have a sufficiently high number of surface cracks. Most critical are just a few cracks.

Considering the magnitude of the surface deformation it has to be stated that this can easily attain a non-negligible and serious amount. For a laminate thickness of $h = 2$ mm and a characteristic neighboring distance of $2d = 40$ mm for example it is predicted that $\Delta w \simeq 8\,\mu$m which may be unacceptable.

On the other hand from the derived results it is clear in which way the unwanted deformation can be reduced. Of course, it can be reduced by use of a thinner laminate. If for some reason (e.g. for sufficient bending stiffness) a relatively thick laminate is required it can be recommended to reduce the individual ply thickness and correspondingly increase the total number of individual plies. The analysis of transverse surface cracks in a thermally loaded cross-ply laminate with more layers (e.g. with $[(90°/0°)_n]_S$-layup) can, in principle, be performed in just the same way as has been demonstrated.

Literature

1. Ehmann, D.; Becker, W.; Salmen, H.: Aspects of Structural Design Optimization for High Precision Reflectors and Mirrors. In: Spacecraft Structures and Mechanical Testing, CNES. Toulouse: Cepadues-Editions 1994, p. 263 – 272.
2. Jones, R. M.: Mechanics of Composite Materials. New York: McGraw-Hill 1975.
3. Salmen, H.; Becker, W.; Abt, B.; Helwig, G.; Egle, W.; Pauschinger, D.: Development and Production of Lightweight CFRP Carriers for the XMM Telescope X-Ray Mirrors. SPIE Vol. 2011 (1993), p. 128 – 137.
4. Tsai, S. W.; Hahn, H. T.: Introduction to Composite Materials. Lancaster: Technomic 1980.

Address: Professor Dr.-Ing. Wilfried Becker, Universität-GH Siegen, Institut für Mechanik und Regelungstechnik, Paul-Bonatz-Straße 9-11, D-57068 Siegen